9.3 COMPARISONS OF LDAR NETWORK HEIGHT AND DENSITY DATA WITH WSR-88D ECHO TOP AND SCIT REFLECTIVITY DATA

Nicholas W. S. Demetriades*, Ronald L. Holle and Martin J. Murphy
Vaisala-GAI Inc., Tucson, Arizona

1. INTRODUCTION

WSR-88D reflectivity data and the algorithms used to help meteorologists interpret these data are extremely important in nowcasting. However, a number of inherent problems arise when tracking thunderstorm cells with 3-dimensional reflectivity. These problems include: (1) Storm Cell Identification and Tracking (SCIT) echo top altitude trends that exaggerate or misidentify thunderstorm growth and decay (Howard et al. 1997), (2) identifying cells in a complex multi-cellular thunderstorm environment, (3) detecting thunderstorm cells at close range from the radar, and (4) volume scans that take 5 minutes to complete. Lightning Detection and Ranging (LDAR) provides another 3-dimensional thunderstorm dataset that has the potential to both complement and supplement WSR-88D reflectivities.

LDAR detects the very high frequency RF pulses (60-66 MHz) that are produced by both cloud and cloud-to-ground (CG) lightning flashes in three dimensions. The median location error for RF pulses detected within the interior of an LDAR network is 250 m. The expected flash detection efficiency of an LDAR network is greater than 95 percent. Another important feature of LDAR is its ability to provide all three dimensions of these data simultaneously and in a continuous datastream. Vaisala-GAI has found that all of these features of LDAR allow it to identify thunderstorm cells and monitor important cell altitude trends very accurately. Lightning altitude trends have already been shown to successfully represent thunderstorm growth and decay in air mass storms (Lhermitte and Krehbiel 1979). A complete description of the Kennedy Space Center (KSC) and Dallas-Fort Worth (DFW) LDAR networks used in this study can be found in Lennon and Maier (1991) and Demetriades et al. (2002), respectively.

This paper will summarize important complementary features that LDAR can provide to radar reflectivity. For some cases of known radar deficiencies, it will be shown that LDAR data could serve as a substitute for radar data.

2. METHODOLOGY

Reflectivity data from the Melbourne, FL and Fort Worth, TX WSR-88D radars were used to make comparisons to the KSC and DFW LDAR networks, respectively. The actual cell identification and echo top trends for the Melbourne WSR-88D were obtained using output from version 3.2 of the SCIT algorithm (Johnson et al. 1998).

LDAR lightning density plots were created in order to identify thunderstorm cells. These density plots were created once every 5 minutes using ~1 km^2 grids. A linear scale was used for displaying the density values. The maximum density value of the linear scale for each plot depended on the location of the storm of interest with respect to the LDAR network and the lightning production of that storm. Density plots were created every 5 minutes because this was the longest time period of lightning that could be displayed before storm propagation and new storm development began to cause lightning contamination from other cells. Another reason for choosing 5 minutes was that it corresponds closely with the length of a WSR-88D volume scan.

After all of the 5-minute LDAR density plots were created for the time period of interest for a particular cell, the lightning from that cell was isolated from lightning produced by nearby cells and merged together into one dataset. The 95^{th} percentile altitude of lightning pulses within the cell was then computed every 2 minutes from this dataset. This served as the lightning top to be used for comparisons with the SCIT echo top.

A number of different methods were used for isolating lightning from a cell of interest for lightning top analysis. Methods that involved all of the RF pulses produced by lightning flashes that initiated within a cell provided some interesting altitude trends, however they appeared to smooth out the growth and decay trends of cells. This was due to long lightning flashes that propagated through adjacent anvils and stratiform rain regions being included with lightning flashes that propagated inside the main convective cores (or main area of interest for storm growth and decay). We obtained better results by analyzing only those lightning pulses located within each storm's convective core. In this approach, we used only those lightning pulses within a certain radius of the center point of a cell. Three different center points were determined for each cell. They were based on the center of the highest ~1, ~4 and ~9 km^2 lightning density areas as shown on the 5-minute lightning density plots. The radius used for trimming lightning around each of these center points was defined as the square root of the area used to determine the center point (i.e. 1, 2 and 3 km). All these analyses represented thunderstorm growth and decay better than the methods described at the beginning of the paragraph, however the lightning top results obtained using the 3 km radius will be the only ones shown in this paper. The 3 km radius was preferred because the 1 and 2 km analyses tended to be noisier. The noise was most likely due to lower lightning pulse numbers for analysis and focusing on an area significantly smaller than the actual convective portion of the cells.

* *Corresponding author address:* Nicholas W. S. Demetriades, Vaisala-GAI Inc., Tucson, AZ 85706-7155; email: nick.demetriades@vaisala.com

3. THUNDERSTORM CELL IDENTIFICATION

3.1 *25 July 1997*

Figure 1 shows a composite reflectivity image of a nonsevere thunderstorm (SCIT cell 1) and adjacent thunderstorms that were identified by SCIT at 2323 UTC 25 July 1997. SCIT performed well by identifying cells 6, 1 and 17 which are clearly visible with reflectivities above 57 dBZ (red). Figure 2 shows the KSC LDAR lightning pulse density plot from the closest 5-minute interval to the radar image in Figure 1. High density lightning cores made cells 6, 1 and 17 easily visible. These two figures demonstrate LDAR's ability to locate cells after they start producing lightning (i.e. become thunderstorms).

Figure 3 shows the difficulty of cell identification within a complex multi-cellular environment using reflectivity data and SCIT. Notice how SCIT misplaced cell 1 as the bottom portion of cell 6. It is not surprising that SCIT was confused because cell 1 is hard to make out visually given the reflectivity pattern. In this situation LDAR complemented radar because the lightning produced by cells 6, 1 and 17 identified three separate and distinct cells (Fig. 4). The highest level of lightning density values (bright pink) has more uniform coverage over the area of the cell than the highest level of reflectivity (red).

3.2 *9 July 1997*

On 9 July 1997 a severe thunderstorm produced dime-sized hail at 2143 UTC. This cell was identified as SCIT cell 2 from the Melbourne WSR-88D reflectivity data (Fig. 5). Although SCIT had cell 2 correctly identified at 2152 UTC, the algorithm identified a new cell (#19) just to its east-northeast. Visually it is hard to identify this reflectivity area as a new cell. Instead, it looks like it is probably part of cell 2. The closest 5-minute LDAR density image shows cell 2 as a large area of high lightning activity but no evidence of a new cell directly to its east-northeast (Fig. 6). Instead, the lightning activity is steadily falling off in that direction. However, LDAR does identify a small, new cell forming about 10 km to the northeast of cell 2. SCIT had not identified this cell as of 2152 UTC (Fig. 5). A visual inspection of Figure 5 demonstrates the difficulty of identifying a new cell in that location based solely on reflectivity data.

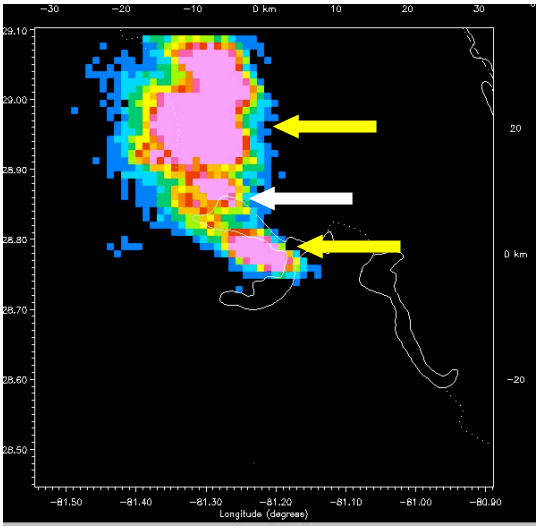

Figure 2. KSC LDAR density image created from lightning pulses detected between 2325 and 2330 UTC 25 July 1997. Bright pink colors represent ≥ 90 lightning pulses per ~1 km^2 grid box. The white arrow points to SCIT cell 1 and the yellow arrows point to SCIT cells 6 and 17.

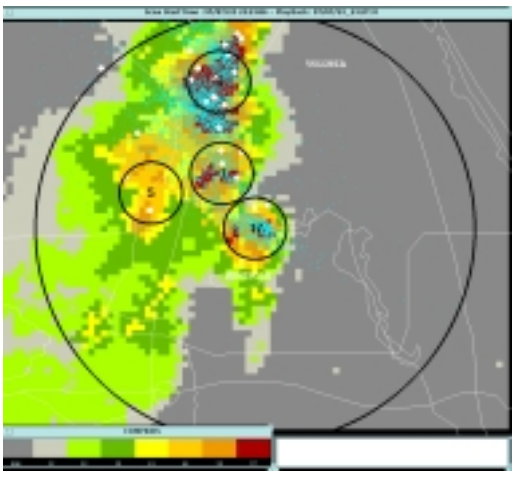

Figure 1. Melbourne, FL WSR-88D composite reflectivity image from 2323 UTC 25 July 1997. SCIT cells are circled and labeled according to cell ID number. The small, light blue dots are LDAR-detected RF pulses.

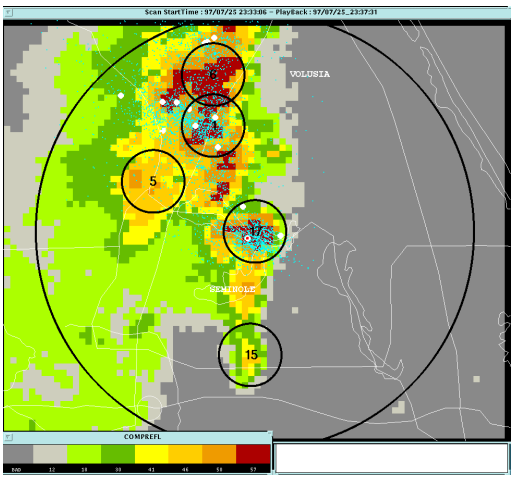

Figure 3. Same as Figure 1, except for 2333 UTC 25 July 1997.

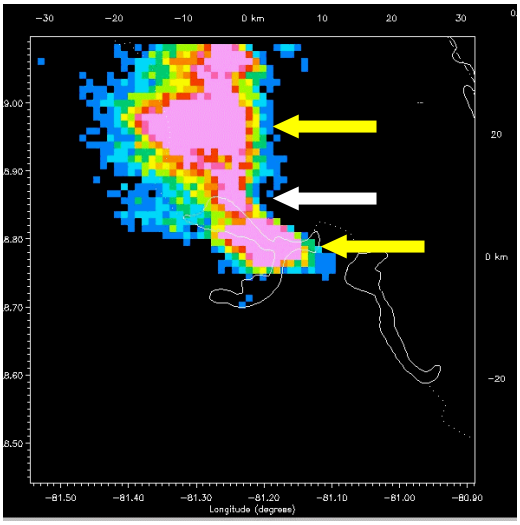

Figure 4. Same as Figure 2, except for KSC LDAR lightning pulses detected between 2335 to 2340 UTC 25 July 1997. Bright pink colors represent ≥ 60 lightning pulses per ~1 km^2 grid box. The white arrow points to SCIT cell 1 and the yellow arrows point to SCIT cells 6 and 17.

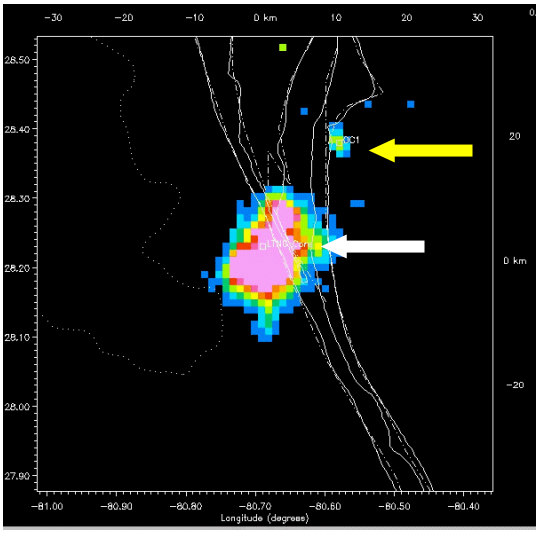

Figure 6. Same as Figure 2, except for KSC LDAR lightning pulses detected between 2150 and 2155 UTC 9 July 1997. Bright pink colors represent ≥ 300 lightning pulses per ~1 km^2 grid box. The white arrow points to SCIT cell 2 and the yellow arrow points to a new cell that developed.

3.3 *6 July 1997*

Another complex multi-cellular thunderstorm environment developed on 6 July 1997. Figure 7 shows a large area of scattered high reflectivity (≥ 46 dBZ) with a well-defined cell that SCIT identified as cell 8. The LDAR density image from the closest 5-minute interval to this radar volume scan clearly identified this cell (Fig. 8). LDAR also detected another cell developing to the northeast of cell 8. SCIT did not identify this new cell yet, probably because it is hard to define a new cell within the reflectivity data at that location. During the next volume scan cell 8 decreases in reflectivity and the cell to its northeast increases in reflectivity (Fig. 9). This caused SCIT to misidentify cell 8 as the new cell that was developing to its northeast. The original cell 8 can be seen visually, however it is not easily identifiable. The LDAR density image from this time clearly shows the original cell 8 and could have prevented this misidentification (Fig. 10).

Figures 9 and 10 also demonstrate the complementary nature of both radar and LDAR datasets. In order for LDAR to identify a cell it must be producing lightning. Figure 10 shows that the new cell located to the northeast of cell 8 did not produce any lightning between 1830 and 1835 UTC. Therefore,

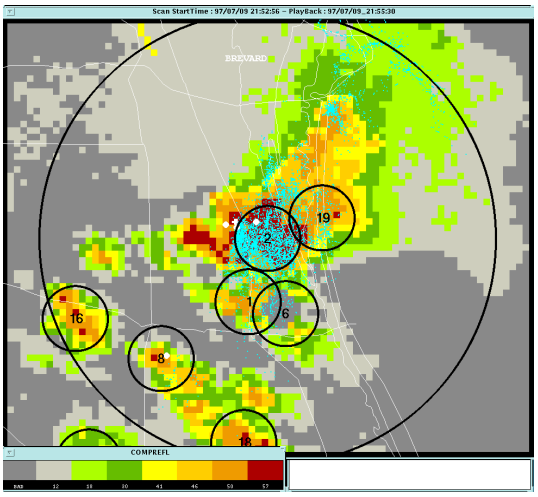

Figure 5. Same as Figure 1, except for 2152 UTC 9 July 1997.

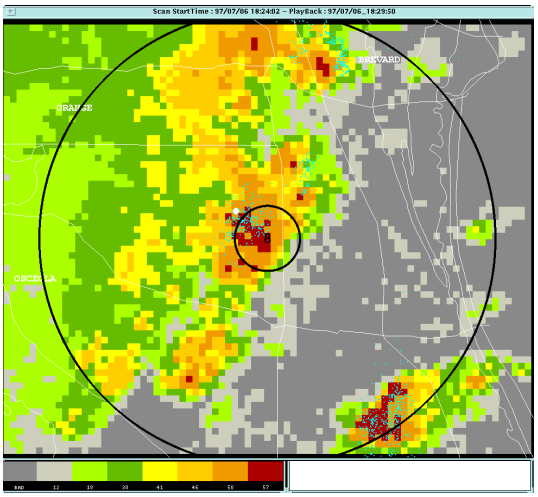

Figure 7. Same as Figure 1, except for 1824 UTC 6 July 1997.

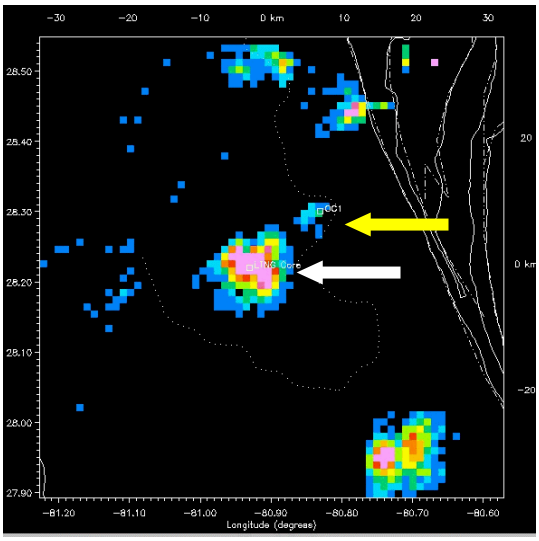

Figure 8. Same as Figure 2, except for KSC LDAR lightning pulses detected between 1825 and 1830 UTC 6 July 1997. Bright pink colors represent ≥ 70 lightning pulses per ~1 km^2 grid box. The white arrow points to SCIT cell 8 and the yellow arrow points to a new cell that is developing to its northeast.

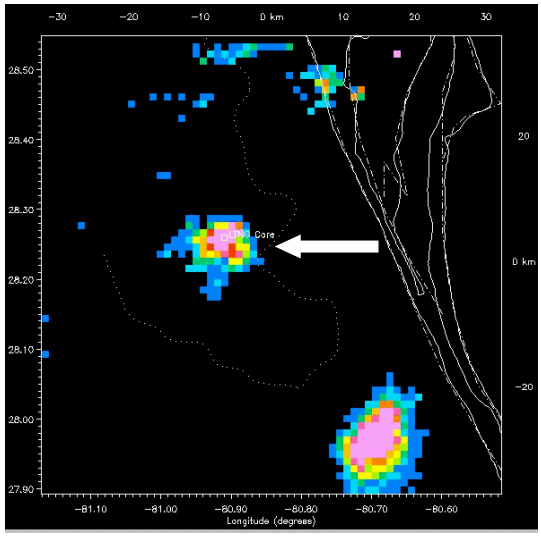

Figure 10. Same as Figure 2, except for KSC LDAR lightning pulses detected between 1830 and 1835 UTC 6 July 1997. Bright pink colors represent ≥ 60 lightning pulses per ~1 km^2 grid box. The white arrow points to the original SCIT cell 8.

radar alone would have identified this new cell that LDAR temporarily lost, and LDAR would have helped radar correctly identify the original cell 8. Figure 11 shows that the new cell quickly reappeared to the northeast in the LDAR image, once it began producing lightning again. LDAR also still shows the original cell 8.

3.4 *23 February 1998*

On 23 February 1998 a severe weather outbreak occurred across central Florida with numerous supercells producing strong tornadoes. One of the supercells that produced an F2 tornado is shown in Figure 12. This cell is easily visible as a large area of reflectivities over 57 dBZ (red) at 0321 UTC. The SCIT algorithm identified it as cell 16. LDAR also clearly shows this supercell as a large area of high lightning

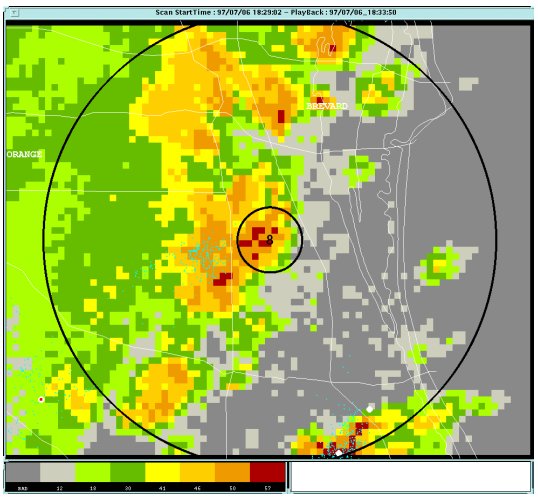

Figure 9. Same as Figure 2, except for 1829 UTC 6 July 1997.

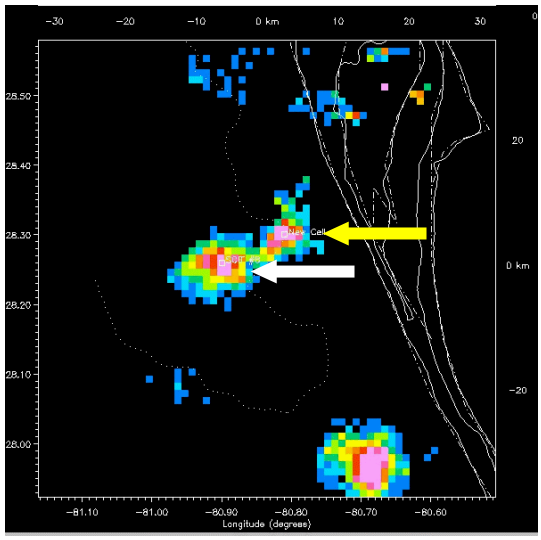

Figure 11. Same as Figure 2, except for KSC LDAR lightning pulses detected between 1835 and 1840 UTC 6 July 1997. Bright pink colors represent ≥ 60 lightning pulses per ~1 km^2 grid box. The white arrow points to the original SCIT cell 8 and the yellow arrow points to the new cell that has developed to its northeast.

density on the 0320 to 0325 UTC density image (Fig. 13). Twenty minutes later SCIT was still tracking cell 16 as one large supercell, however LDAR now showed two distinct lightning cores (Figs. 14 and 15). A visual inspection of the composite reflectivity data shows no evidence of a second, adjacent cell.

3.5 *15 June 2001*

Early on 15 June 2001 a strong squall line passed through the DFW area. This squall line produced baseball-sized hail and wind gusts over 70 mph (113kph) as it moved through north Texas. Figure 16 shows the base reflectivity data from the Fort Worth WSR-88D at 0054 UTC. The leading convective portion of the squall line is delineated by a fairly uniform line of reflectivities over 45 dBZ. This case demonstrates how difficult it is to distinguish individual cells within a squall line using base reflectivity. A 5-minute LDAR II density image from this time shows the highest lightning density cores along the leading convective portion of this squall line and lower lightning densities where flashes occasionally propagated through the trailing stratiform rain region (Fig. 17). This is a typical example of LDAR II's ability to identify individual cells within convective portions of squall lines. Notice that at least 5 separate cells can be identified within the line.

4. RADAR ECHO TOP AND LDAR LIGHTNING TOP COMPARISONS

4.1 *25 July 1997*

The echo top and lightning top data for this case came from the nonsevere thunderstorm (SCIT cell 1) that was discussed earlier in Section 3.1. Figure 18 shows the echo tops and lightning tops from this case. This cell started at a distance of ~110 km to the northwest of the Melbourne WSR-88D and propagated toward the northeast. The echo top that SCIT calculated from this storm began at 12 km and then

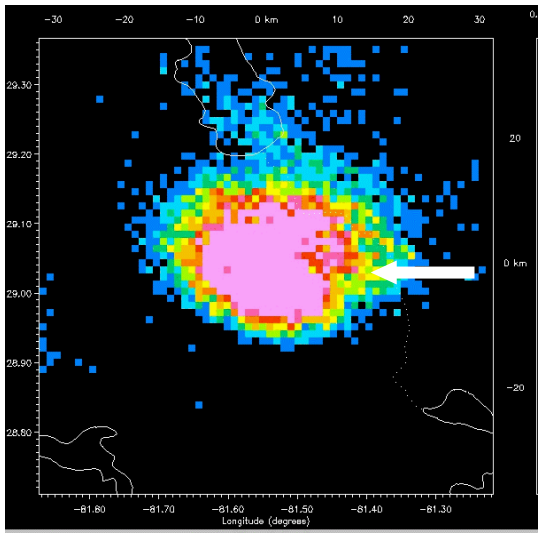

Figure 13. Same as Figure 2, except for KSC LDAR lightning pulses detected between 0320 and 0325 UTC 23 February 1998. Bright pink colors represent ≥ 30 lightning pulses per ~1 km^2 grid box. The white arrow points to SCIT cell 16.

quickly started a rapid descent. Between 2317 and 2327 UTC the echo top fell from 12 to 4 km and then rose to 12.5 km at 2332 UTC. Part of this descent is probably real because the lightning top initially starts to descend around 2317 UTC. However, the continued descent to 4 km and rapid rise to 12.5 km are exaggerated representations of this storm's growth and decay. This exaggerated drop and ascent is likely caused by the storm moving through different tilts of the radar volume scan at long range. By 2321 UTC, the lightning top was already increasing again and radar reflectivities were growing within the cell (not shown). In fact, the lightning top remained at a fairly constant altitude (~14 km) while the echo top descended to 4 km

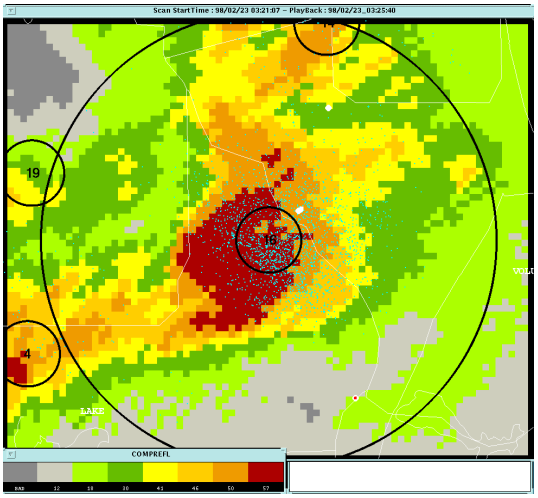

Figure 12. Same as Figure 2, except for 0321 UTC 23 February 1998.

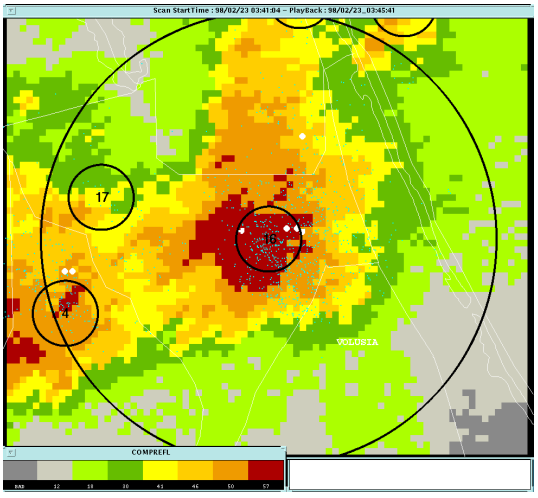

Figure 14. Same as Figure 2, except for 0341 UTC 23 February 1998.

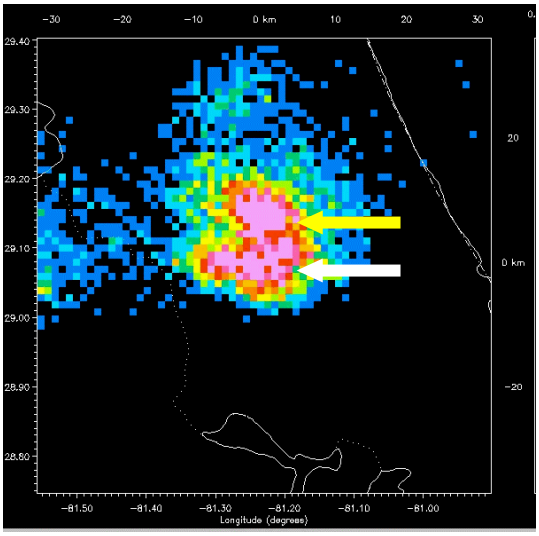

Figure 15. Same as Figure 2, except for KSC LDAR lightning pulses detected between 0340 and 0345 UTC 23 February 1998. Bright pink colors represent ≥ 30 lightning pulses per ~1 km^2 grid box. The white arrow points to SCIT cell 16 and the yellow arrow points to the new lightning core that developed just to its north.

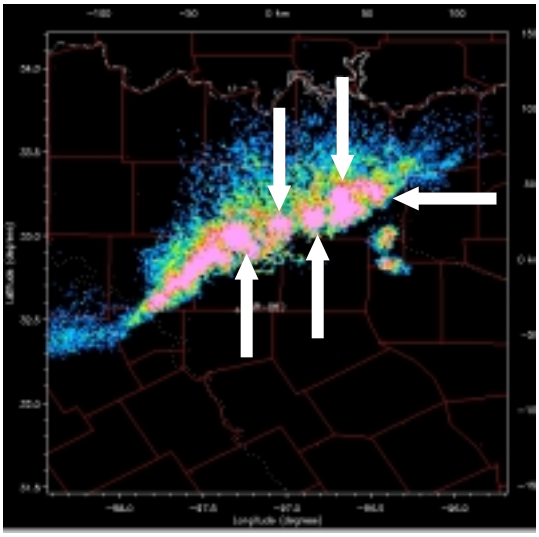

Figure 17. Same as Figure 2, except for DFW LDAR II lightning pulses detected between 0051:30 and 0056:30 UTC 15 June 2001. Bright pink colors represent ≥ 20 lightning pulses per ~1 km^2 grid box. The white arrows point out five individual convective cells within the squall line.

and then rose again to 12.5 km. By 2337 UTC, the echo top did not even belong to the proper cell anymore because of SCIT's misidentification (see Section 3.1).

4.2 *9 July 1997*

The severe thunderstorm examined in this case is the dime-sized hail producer discussed in Section 3.2. Figure 19 shows the echo top and lightning top analysis for this storm. At 2107 UTC, this cell was located ~50 km due north of the Melbourne WSR-88D. During the next hour, it propagated due south and moved into the WSR-88D cone of silence. This is clearly evident from the echo top analysis that shows a gradual descent from 12 km at 2107 UTC to 3 km at 2152 UTC. The lightning top analysis initially shows a slight ascent and then levels off at ~14 km until 2134 UTC. The radar reflectivities also remained consistently high between 2107 and 2134 UTC (not shown). After 2134 UTC, the lightning tops gradually ascended until they reached 15.5 km at 2146 UTC. The radar reflectivities also increased during this time period. During the lightning top ascent, the storm began producing dime-sized hail at 2143 UTC.

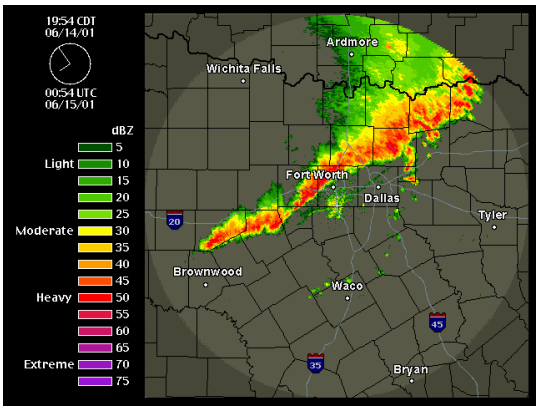

Figure 16. Fort Worth, TX WSR-88D base reflectivity image from 0054 UTC 15 June 2001.

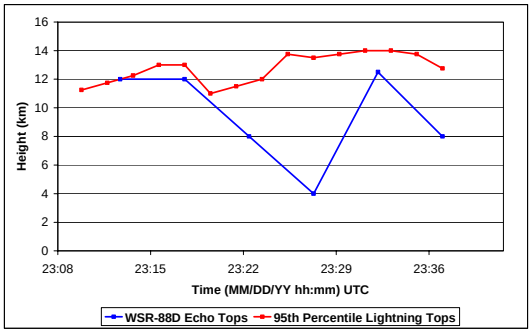

Figure 18. SCIT echo top trends obtained from the Melbourne, FL WSR-88D and lightning top trends calculated from the KSC LDAR network for the nonsevere thunderstorm (cell 1) that developed on 25 July 1997.

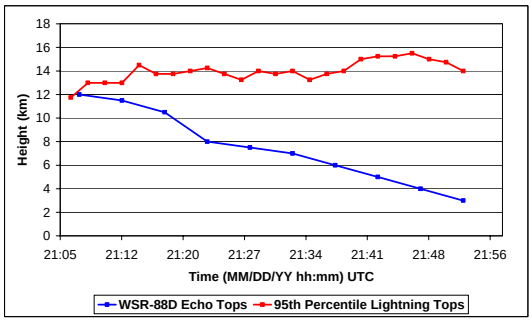

Figure 19. Same as Figure 18, except for the severe thunderstorm that produced dime-sized hail at 2143 UTC 9 July 1997.

4.3 *31 July 1997*

The 31 July 1997 storm was initially ~110 km to the northwest of the Melbourne WSR-88D and then propagated to the east-southeast, toward the radar. Figure 20 shows the echo and lightning top analysis from this case. Both the echo and lightning tops from this storm initially ascended until about 2008 UTC. Then the echo tops descended from 12 to 8 km and then rose again to 11 km during the next two volume scans. During this time period, the lightning tops descended slightly, but were mostly between 12 and 13 km. After 2019 UTC the lightning and echo tops are in fairly good agreement with both showing ascents as the cell's reflectivity increased (not shown). The echo top rise in altitude from 8 km at 2014 UTC to 15 km at 2024 UTC would correspond to an effective upward velocity of about 12 ms^{-1}. Although this is a reasonable updraft velocity, would the 30 dBZ echo top rise at this rate? After comparing lightning and echo top cases such as those discussed in sections 4.1 and 4.2, this might be another case of exaggerated storm growth and decay. If it was exaggerated storm growth and decay, it was most likely caused by the storm's real echo top sliding down one radar tilt between 2009 and 2014 UTC until it intercepted a new one at 2019 UTC, as the storm moved closer to the radar.

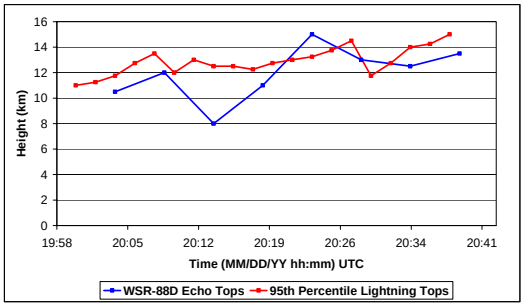

Figure 20. Same as Figure 18, except for severe thunderstorm that produced dime-sized hail at 2035 UTC 31 July 1997.

5. SUMMARY

Comparisons of LDAR with WSR-88D reflectivity data show that LDAR can complement and, at times, supplement radar reflectivity data for thunderstorm cell identification and growth and decay trends. The case studies examined in this paper demonstrate LDAR's ability to identify and track thunderstorm cells more accurately in complex multi-cellular thunderstorm environments. Two major reasons are (1) LDAR's higher spatial resolution relative to WSR-88D, and (2) the fact that maxima in lightning activity aloft appear to be closely associated with convective cores only. LDAR data also showed great temporal continuity that not only aids in identifying cells but also potentially tracking them.

Altitude analyses from a number of storms showed that lightning altitude trends can provide a large improvement over SCIT echo top trends for tracking thunderstorm growth and decay. Exaggerated SCIT altitude trends were probably partially due to echo tops from cells moving between different vertical tilts of the radar beam. Other echo top misrepresentations were due to storms approaching the radar and gradually being caught in the cone of silence. Finally, the continuous data stream provided by LDAR allowed lightning altitude trends to be tracked on smaller time scales than the 5-minute updates of WSR-88D. This provided a higher level of detail for both thunderstorm growth and decay.

6. FUTURE WORK

Vaisala-GAI will be continuing to study thunderstorm cell identification and altitude trends using LDAR and radar reflectivity in order to address many of the issues raised by this study. Radar reflectivity data on constant altitude surfaces aloft will be used to further examine the possibility that LDAR defines individual cells better within certain thunderstorm environments because most of the lightning it detects is aloft. SCIT or a functionally similar cell-tracking algorithm will be run with LDAR density data to find out if SCIT really can identify individual cells better within complex multi-cellular thunderstorm environments using LDAR as a complement to radar reflectivity. Another area of study will involve examining three dimensional radar reflectivity data to try to identify what is causing the divided lightning cores found within supercells.

7. REFERENCES

Demetriades, N.W.S., M.J. Murphy and K.L. Cummins, 2002: Early results from the Global Atmospherics, Inc. Dallas-Fort Worth lightning detection and ranging (LDAR-II) research network, *Preprint, 6th Symposium on Integrated Observing Systems*, Orlando, FL, Amer. Meteor. Soc., 202-209.

Howard K.W., J.J. Gourley and R.A. Maddox, 1997: Uncertainties in WSR-88D measurements and their impacts on monitoring life cycles, *Wea. Forecasting*, **12**, 166-174.

Johnson, J.T., P.L. MacKeen, A. Witt, E.D. Mitchell, G.J. Stumpf, M.D. Eilts, and K.W. Thomas, 1998: The storm cell identification and tracking algorithm: An enhanced WSR-88D algorithm, *Wea. Forecasting*, **13**, 263-276.

Lennon, C., and L. Maier, 1991: Lightning mapping system, *Proceedings of the International Aerospace and Ground Conference on Lightning and Static Electricity*, Cocoa Beach, FL, NASA Conference Publication 3106, Vol. II, 89.1-89.10.

Lhermitte, R., and P.R. Krehbiel, 1979: Doppler radar and radio observations of thunderstorms, *IEEE Trans. Geosci. Electon.*, *GE-17*, 162-171.